

CONTAMINATION MECHANISMS  
OF  
SOLID ROCKET MOTOR PLUMES

M. K. Barsh  
J. A. Jeffery  
P. Brestyanszky  
K. J. Adams

Aerojet ElectroSystems Company  
Azusa, California

## Contamination Mechanisms of Solid Rocket Motor Plumes

M. K. Barsh, J. A. Jeffery,  
P. Brestyanszky, and K. J. Adams

Aerojet ElectroSystems Company  
Azusa, California

A new generation of space satellites require freedom from contamination upon insertion into final operational orbits. There is concern that the combustion plume from solid rocket motors (SRMs) such as the Inertial Upper Stage (IUS) units, which will be employed to deliver payloads into space after deployment from the STS shuttle craft, may be a source of significant contamination.

Although the payloads are located forward of the SRMs, evidence has been uncovered that suggests that recirculation of nominally trivial amounts of plume products flowing  $180^\circ$  to the direction the rocket exhaust occurs during the rocket firing and, further, that these recirculated products can and will deposit on sensitive thermal control surfaces of the payloads to degenerate their effectiveness.

In order to assess this phenomenon, several mechanisms were postulated which might explain how the recirculation could occur. These are:

1. Charge separation - the plume products assume a charge opposite to the SRM and/or payload structures by virtue of triboelectric effects or thermal ionization.
2. Intra-plume collision - some faster moving species collide with slower moving ones, resulting in a vector velocity counter to the plume direction.
3. Nozzle boundary layer effects - exhaust product flow at the nozzle wall-plume interface results in a boundary layer that conforms to the nozzle surface and ultimately flows in direction counter to the plume direction.

Preliminary analytical computer models describing those mechanisms have been developed and experimental verification of the phenomena has been explored.

## 1.0 INTRODUCTION AND SUMMARY

The NASA Space Transportation System (STS) which consists of the shuttle stage and the solid rocket motor (SRM) Inertial Upper State (IUS), will carry some payloads whose performance can be compromised by the accumulation of thermo-optically contaminating deposits. Whereas significant efforts to evaluate the contamination potential of the shuttle system have been made, no concern for the contamination potential of the SRM firings of the IUS have been explored. It has generally been assumed that since the payloads will reside well forward of the exit nozzle of the IUS systems that no rocket plume products could find their way to the critical areas of the payloads.

Aerojet ElectroSystems Company (AESC) elected to investigate the possibility of contamination from the IUS motor firings since prior studies of some of their payload systems slated for STS launchings had established that a homogeneous deposit of as little as 0.1 gm of material on some critical areas ( $<1.0 \times 10^{-6}$  gm/cm<sup>2</sup>) could degrade the system performance unacceptably. Since the first stage IUS propulsion products will weigh approximately 10,000 Kg, a deposit of 1 part in 100,000,000 derived from the SRM's could constitute a serious problem.

A survey was made of SRM launches in the past and a number of cases were uncovered which clearly suggested that "recirculation" contamination was a reality.<sup>1</sup> The nature of the evidence ranged from the increase in the optical absorptance ( $\alpha$ ) of thermal control surfaces to the presence of "convective" base heating caused by phenomena other than plume

1. Maag, Carl R., Backflow Contamination For Solid Rocket Motors, presented at the USAF/NASA International Spacecraft Contamination Conference, Colorado Springs, Colorado (1978).

radiation upon SRM firings. The conclusion, deduced from the evidence that strongly points to exhaust products migrating forward and adhering to the payload sites, is counter-intuitive in view of the opposite velocity vectors of the main mass of the burn products. Yet this concept or related ancillary phenomena have received superficial consideration by other investigators. Thus, for example, Boynton<sup>2</sup> recognized that the exhaust gases occurring at the large turning angles of a rocket engine at high altitudes, have density distributions far different from those of the far field plume. This has been supported by the work of Simons<sup>3</sup> and Pearce<sup>4</sup>. Further, in discussing the possible effects of the nozzle boundary layer on plume expansion, Arnold<sup>5</sup> stated that some flow can expand around the nozzle exit and flow back up the outside of the nozzle. Suebold<sup>6</sup> confirms that subsonic flow next to the nozzle wall is capable of making a complete 180-degree turn and head back upstream. Martinkovic<sup>7</sup> expressed the same idea. Apparently, however, no attempts to quantize the mass fluxes resulting from such backflow were made\*. Nor were any possible explanatory physical mechanisms formulated. Recently,

2. Boynton, F.P., Exhaust Plumes From Nozzles With Wall Boundary Layers, Journal of Spacecraft & Rockets, 5:1143-1147 (1968).

3. Simons, G.A., Effect of Nozzle Boundary Layers in Rocket Exhaust Plumes, AIAA Journal, 10:1534-1535 (1972).

4. Pearce, Blain E., An Approximate Distribution of Mass Flux In A High Altitude Solid Propellant Rocket Plume, AIAA Journal, 12:718-720 (1974)

5. Arnold, F., An Experimental Method For Locating Stream Tubes in A Free Jet Expansion to Near Vacuum, AEDC-TR-69.17.

6. Seubold, Jason G., Edwards, R.H., A Simple Method For Calculating Expansion of A Rocket Engine Nozzle Boundary Layer Into A Vacuum, Hughes Co.

7. Martinkovic, P.J., Bipropellant Attitude Control Rocket (ACR) Plume Contamination Investigation AFRPL-TR-69-261.

Chirivella<sup>8</sup> has reported experimental mass flux data in nitrogen and carbon dioxide from a series of five conical nozzles for angles extending beyond  $100^{\circ}$  relative to the nozzle centerline. Results indicated significant mass flux in the backflow region. Calia and Brook<sup>9</sup> supported these findings by confirming in their tests, substantial mass flux levels in the neighborhood and beyond the limiting Prandtl-Meyer characteristic. These flux levels were several orders of magnitude larger than predictions from inviscid flow theory.

In order to attempt to resolve the question of recirculation contamination from the IUS SRM's, an analytical model study was initiated. Three independent mechanisms were postulated for the steady-state burn and were studied using available literature data. An attempt has been made to predict, with the aid of these preliminary analytical models, the recirculation of potential contaminants forward to the site of a typical payload from SRM-1 (the larger of the two IUS motors). The modeling studies and the results and conclusions are described below.

## 2.0 BACKGROUND

Solid rocket motor firings have been studied and the following observations are pertinent. At start-up, the SRM generates a small amount of unburned products for a very short time until the SRM chamber pressure builds up. The major portion of the burn, steady-state, occurs at high temperature and pressure and essentially complete combustion is achieved (for stoichiometric propellant compositions). At shut-down, significant amounts of partially burned products are evolved as the pressure and

8. Chirivella, Jose E., Molecular Flux Measurements In The Back-flow Regions Of A Nozzle Plume, Tech memo 33-620, 1973, JPL.

9. Calia, U.S., and Brook, J.W., Measurements Of A Simulated Rocket Exhaust Plume Near The Prandtl-Meyer Limiting Angle, Journal Spacecraft and Rockets, 12(No. 4): 205-208 (1975).

temperature decay. However, since most of the propellant combustion products occur during the steady-state phase and since this phase was most amenable for analysis, the analytical efforts were directed at the steady-state-burn plume products.

Three mechanisms analyzed for the recirculation of contamination from the SRM plumes of the IUS were:

1. Charge separation
2. Collisional
3. Boundary flow

For purposes of expediency in simplifying the mathematical derivations and computer programs, it was assumed that the three mechanisms were independent and that the results would be additive. It is, of course, evident that if the three mechanisms are viable, they must be operative concomitantly and that eventually they will have to be integrated to provide a more realistic prediction of the contamination potential. The more remote, (from targets of interest) but larger of the two IUS motors (SRM-1) was selected for study because it represented a conservative case.

The "charge separation" mechanism was conceived as the consequence of two separate phenomena: (1) triboelectric effects developed by the very high velocity particles ejected from the nozzle and (2) thermal ionization of the ejected species by virtue of the high temperatures of the burning propellant. Illustrative of the former phenomenon are references to potentials estimated up to a half million volts<sup>10, 11</sup> and

10. Fristrom, R.M., Oyhus, F.A., and Albrecht, G.H., Charge Buildup on Solid Rockets As a Frame Burst Mechanism, ARS Journal, 32:1729-1730 (1962).

11. Nanevich, J.E., and Hilbers, G.R., Titan Vehicle Electrostatic Environment, Technical Report AFAL-TR073-170, July 1973.

average number of electrons in the plume of  $10^{10} \text{ e/cm}^3$ <sup>12</sup>. With reference to the latter phenomena, thermodynamic predictions of the thermal ionization of species such as



+



etc.

support the premise. If it is assumed that the net results of the phenomena is to provide a charge separation effect, then the plume might be envisioned as taking on one charge and the spacecraft (and payload) the opposite charge. This, then, could provide one driving mechanism for the recirculation of some of the plume products (see Figure 1A).

The collisional mechanisms were an outgrowth of a microcosmic consideration of the burn history of a typical SRM. First, it is clear that when combustion occurs at the solid combustion plume interface, explosion and ejection from the surface of various sized burning propellant pieces occur. As these are subsequently ejected out of the nozzle, they continue burning and are ultimately consumed. Yet, some of the larger particles have been observed to still be burning even after they have left the nozzle. This indicates a distribution of velocities and sizes of ejected species in the plume. This then suggests the possibility of larger, slower moving particles in the plume being impacted by smaller, faster moving particles which can then rebound and provide a source of

12. Smith, Felix T., and Gatz, Carole R., Chemistry of Ionization in Rocket Exhausts, Paper presented at the ARS Ions in Flows and Rocket Exhausts Conference, Palm Springs, CA. (1962).

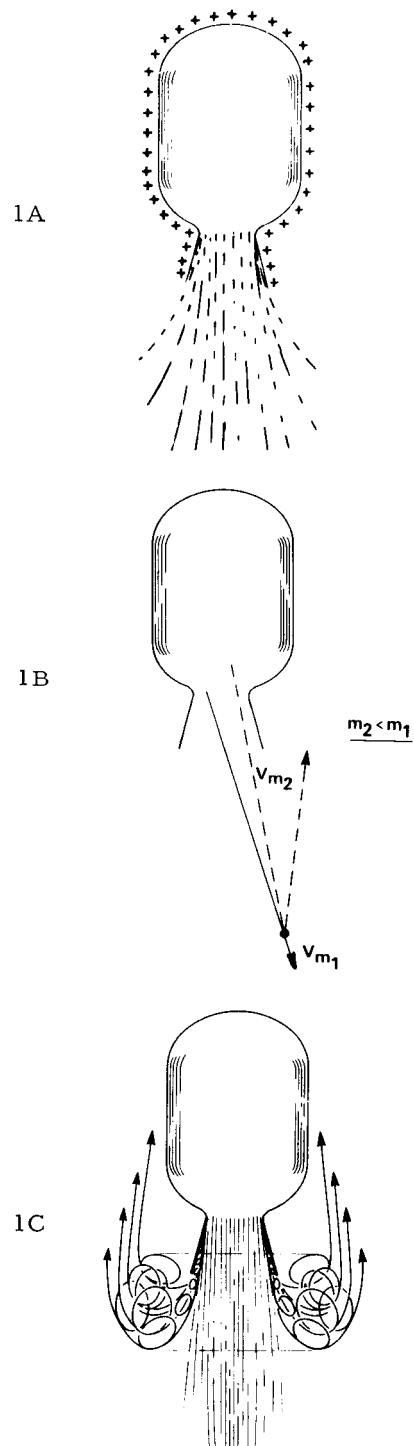


FIGURE 1 CONTAMINATION RECIRCULATION MODELS



recirculation contamination (see Figure 1B). It is noteworthy that the classical inviscid flow Prandtl-Meyer expansion of a plume into a vacuum has been studied and has been able to predict plume products up to as far as  $120^\circ$  from the axis of the rocket. But, attempts to analyze the plume rigorously were unsuccessful even though theoretical considerations clearly state that a  $180^\circ$  recirculation was possible<sup>14</sup>. An alternate approach involving a statistical approach was subsequently selected and is described in the analytical sections.

The "boundary flow" mechanism was postulated because of the recognition that the nozzle wall boundary turbulence was at once a possible explanation for slower moving species in the plume and for a way in which the species could "turn the corner." Previous work at Lockheed Aerospace Corporation<sup>15</sup> gave some insight into how these phenomena could occur but the analysis was only carried to indicate species up to approximately  $120^\circ$  from the axis of the rocket. Since an explanation for recirculation in the  $120^\circ$  to  $180^\circ$  range was sought, an approach was invoked which identified three possible sources of rearward flowing material which could be formulated analytically. First, the presence of a shock wave and the related base-flow, boundary layer separation was assumed per Weinbaum et al.<sup>13</sup> Next, the effect of the nozzle turbulent boundary-layer on mass fluxes beyond the theoretical limiting angle was considered. Finally, the existence, in the vicinity of the nozzle exit, throughout the firing period, of a torus or vortex ring of particles experiencing high rotations, was formulated. The subsequent dissipation of this "doughnut" of particles then gave rise to a vector distribution of particle velocities some of which were oriented so as to provide a continuous source of material for recirculation contamination (see Figure 1C).

13. Weinbaum, Sheldon and Weiss, Robert F., Hypersonic Boundary Layer Separation and the Base Flow Problem, AIAA Journal, 4 No 8: 1321-1330 (1966)

14. Grimson, J., Advanced Fluid Dynamics and Heat Transfer, McGraw Hill, 1971.

15. Private communication with M. Fong et al, Lockheed Missiles and Space Division, Sunnyvale, CA.

In the following section, a more detailed description is provided of the way in which the three mechanisms were formulated. The description will include an identification of the analysis flowcharts utilized to make the recirculation contamination predictions. The input data used for these models is summarized in Figures 2, 3, and 4.

### 3.0 ANALYTICAL MODELS

#### 3.1 Charge Separation

The objective of the charge separation model is to predict recirculation flux of particles from the solid rocket plume due to electric fields. These electric fields have been studied extensively and arise from charging effects due to thermal ionization and triboelectric processes.<sup>11,12,16,17</sup> The charge builds up on the spacecraft surface and exerts a force on any charged particles in the plume. The force can be substantial enough to explain a significant return flux of particles which impinge on sensitive satellite surfaces.

In order to model the process, some assumptions had to be made. The return flux is obviously dependent on several of the parameters in question. For instance, the greater the velocity of the particle, the greater its probability of escaping the pull of the electric fields, but the greater the charge on the particle the greater its probability of

16. Cole, B.N., Baum, M.R., Mobbs, F.R., An Investigation Of Electrostatic Charging Effects in High-Speed Gas-Solids Pipe Flows, Proceedings of The Institute of Mechanical Engineers, 184 (pt. 3C): 77-83 (1969).

17. Maise, George, and Sabadell, Alberto J., Electrostatic Probe Measurements In Solid Propellant Rocket Exhaust, AIAA Journal, 8 (No. 5): 895-901 (1970).

## INPUT DATA

### Engine Specifications:

	Max. Propellant Weight	21,400 lbs
	Expended Inerts	214 lbs
	Total Impulse	6,266,000 lbs
	$I_{sp}$ (effective)	292.35 sec.
	Burn Duration	156 sec.
	Chamber Pressure	$P_c = 600$ psi
Nozzle	{ Throat Diam.	6.25 in.
	{ Exit Diam.	56.5 in.
	$\gamma = 1.12$	
	Exit Mach No.	$M = 4$

FIGURE 2

<u>Fuel Composition</u>	<u>% Wt</u>
$NH_4ClO_4$	68%
Al	18%
$C_{11}H_{26.6}O_{.2}$ (Binder)	12.94%
$C_{22}H_{42}O_4$ (Cat.)	1.06%

FIGURE 3

INPUT DATA (Continued)

<u>Constituent</u>	<u>Wt %</u>
$\text{Al}_2\text{O}_3$	34.02
CO	26.27
$\text{CO}_2$	3.01
Cl	.001
H	.0001
HCl	21.11
$\text{H}_2$	2.76
$\text{H}_2\text{O}$	4.72
$\text{N}_2$	8.11

FIGURE 4 PRODUCTS OF COMBUSTION

recirculating. Greater particle mass also increases escape probability, and other factors influence this probability to a lesser extent. In light of this it is seen that recirculation is very sensitive to particle parameters. Thus an effort must be made to determine accurately the distribution of all these parameters, and fit Gaussian distributions to them for use in a random number computer subprogram. It was found that the particle size distribution in the plume could be described by a dual Gaussian distribution with peaks about the means of  $.1\mu$  and  $.3\mu$ .<sup>18</sup> The  $.3\mu$  peak had 80% of the amplitude of the  $.1\mu$  peak and their standard deviations were  $.1\mu$ . In order to simulate this curve in the computer program five particles were chosen from the  $.1\mu$  distribution for every four particles chosen from the  $.3\mu$  distribution. The velocity of the particles was calculated to be normally distributed about an average of 3688 meters/second with a standard deviation of 1000 meters/second and normally distributed in a mean direction of  $0^\circ$  with respect to the longitudinal axis and a sigma of  $16^\circ$ .<sup>19,20</sup> The charges on the particles were chosen to be normally distributed about an average of 10 electrons and a standard deviation of 10 electrons.<sup>12</sup> The final distribution describes the radial position at which the particle leaves the nozzle. When preliminary computer runs revealed that the return flux was relatively insensitive to choice of radial position, a radial position distribution was selected as an initial working value. This distribution described more particles as originating at the center of the nozzle with less emanating closer to the nozzle wall. Thus the distribution was chosen to have an

18. Personal communication with E. Borson, Aerospace Corp., Nov. 1977.

19. Kliegel, James R., Gas Particle Nozzle Flows, Chemical Reactions and Phase Changes in Supersonic Flow.

20. Hoffman, R.J. et al, Plume Contamination Effects Prediction: The CONTAM Computer Program Version II, AFRPL-TR-73-46 (1973) Final Report, Contracts F04611-70-C-0076 and F04611-72-C-0037, McDonald Douglas Astronautics Corp.

average radial position of zero and a standard deviation numerically equal to the nozzle radius, .72 meters. Other assumptions in the computer analysis are that the rocket is in steady state operation, the charge distribution over the spacecraft is uniform and the spacecraft is modeled as 6 cylinders atop one another representing different segments of the entire spacecraft (Figures 5, 6). In order to keep the model as conservative as possible,  $\text{Al}_2\text{O}_3$  was chosen from the thermodynamically calculated table of combustion products (Figure 4) to represent the contaminants. Although it is realized that some unidentifiable condensates must also be present in the exhaust products contamination, it was felt that the high density of  $\text{Al}_2\text{O}_3$  would keep our results conservative. It was also felt that most of the gaseous products would not adhere to satellite surfaces, even at low temperatures, whereas  $\text{Al}_2\text{O}_3$  particles, once they adhered, would tend not to re-emit. For these reasons,  $\text{Al}_2\text{O}_3$  particles were chosen as representative of the return flux and contaminants.

The modeling approach was to randomly choose a particle according to the distributions above and then step the particle through a series of time increments in order to trace its trajectory. The particle is never allowed to travel more than one meter before its position, velocity, and the force acting upon it are recomputed. Thus the entire trajectory of the particle relative to the rocket is described and its impingement location recorded. The masses of the impinging particles are summed to give the total mass contamination on the surfaces of the satellite and the rocket. These numbers are further divided by the areas of the sensor and rocket respectively to give the density of contamination in  $\text{g/cm}^2$ . In order to save computation time the escape energy divided by the charge was used to predict, a priori, what particles would not return and these were rejected from consideration and not calculated. In terms of the Gaussian distributions, the following relation was derived from the equation of motion:

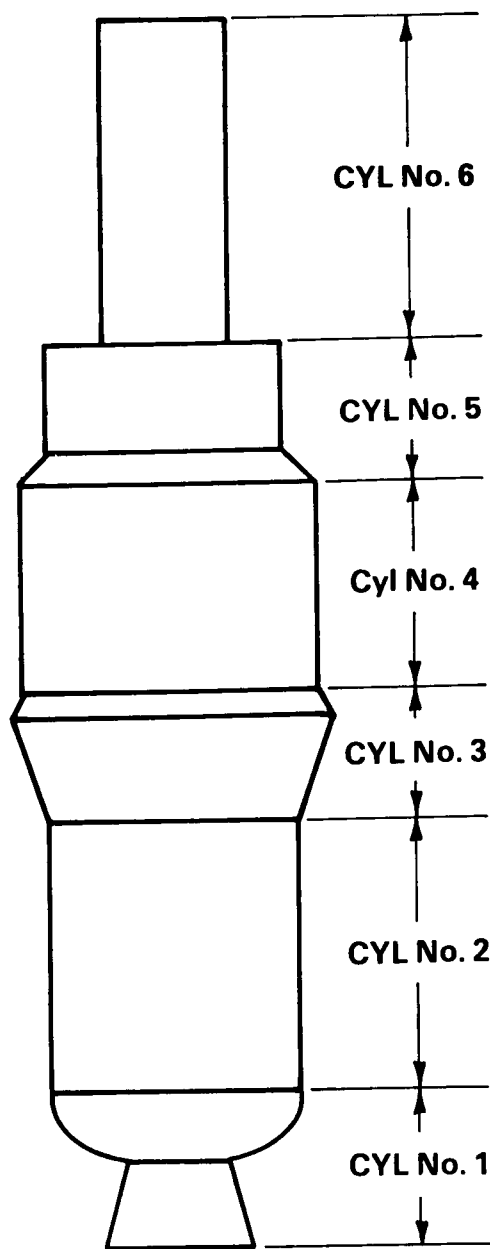


FIGURE 5 SPACECRAFT MODEL

Cylinder No.	Diameter (cm)	Length (cm)
1	213.36	149.86
2	231.14	251.46
3	289.56	119.38
4	277.88	203.20
5	218.95	114.30
6	114.30	304.80

FIGURE 6 DIMENSIONS OF IDEALIZED CYLINDRICAL SURFACES



$$\frac{mv^2}{Q} \leq \frac{4}{3} \pi \frac{(r-\sigma_r)^3 (v-\sigma_v)^2}{Q + \sigma_q} \quad (3)$$

where the  $\sigma_x$ 's are the standard deviations of the distributions of their subscripts (r refers to particle radius, v to velocity, and q to charge). Thus only particles satisfying this relationship would be calculated by the iterative approximation of the trajectory described above. The analysis flowchart is indicated in Figure 7.

The trajectories and impingement locations were printed by the computer for every particle, and it was observed that most particles with high charge tended to recombine in the plume while particles of large mass because of their energy (the force being charge dependent and not mass dependent) tended to escape, as was the case of particles with large velocity. Thus particles with low mass and velocity and low average charge tended to recirculate (sometimes in rather large arcs) to impinge on the modeled surfaces. More generally tended to impinge on the surfaces closer to the nozzle, the probable explanation being their proximity to the plume and its greater charge due to its larger area (the surface charge distribution being assumed to be constant as a first approximation). The impingement results are summarized in Figure 10 in terms of gm/cm<sup>2</sup>.

The model is limited, of course, by its calculation of finite elements of the trajectory and the input data and assumptions. The assumption that the electrical effects act independently of the vortex turbulence and collisional processes is the most obvious one that will have to be eliminated in further contamination studies. The model will have to couple the effects of all three in order to give an accurate

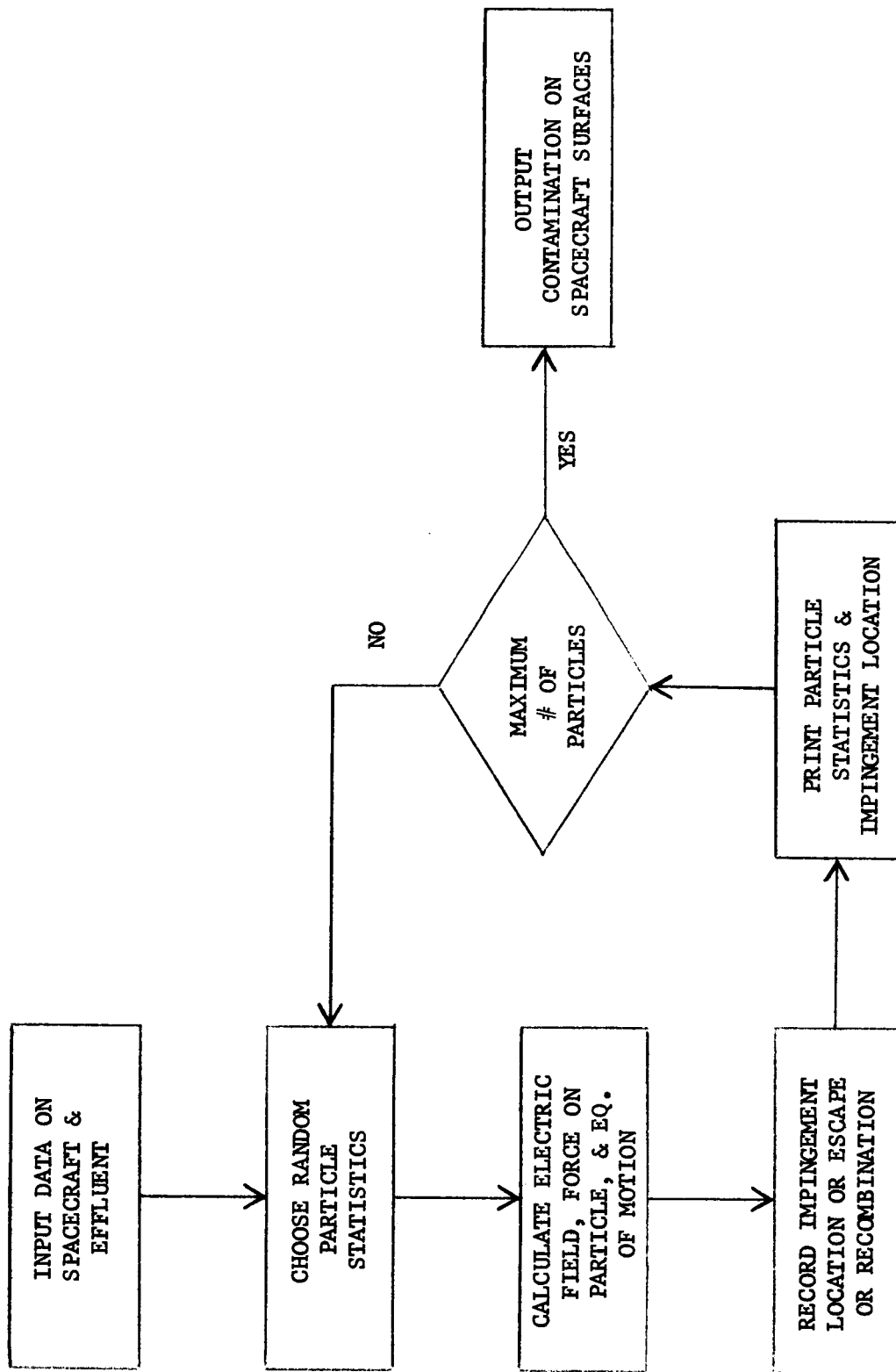


FIGURE 7 CHARGE SEPARATION ANALYSIS FLOW CHART

account of what is going on in the plume. Better distributions for particle velocities, charges, and densities will be obtained as the engine is tested and experiments are done. Better data on the effluents and the magnitude of the engines' charging effects will also be obtained and included in future modeling efforts.

### 3.2 COLLISIONAL

Of primary interest in the dynamics of Rocket Plumes is the manner in which the intermolecular and interparticle collisions influence the flow fields. Collisional processes were postulated to be a possible mechanism by which recirculation occurs. In order to facilitate the calculations involved in such a model, some plausible assumptions had to be made. The first of these involved the particle size distributions and were based upon calculations done as part of plume impingement studies at NASA MSFC<sup>21</sup>. A bimodal Gaussian size distribution was assumed with a mass fraction of .55 for submicron particles with an average size of  $.178\mu$  and a mass fraction of .45 for micron particles with an average size of  $1.78\mu$ . The geometry of the spacecraft was modeled as six cylinders atop one another representing the different segments. Start-up and shut-down transients were ignored and only steady state operation was investigated. The particle density in the plume was assumed to have a  $1/r^2$  dependence in distance from the nozzle and be limited by the  $16^\circ$  maximum cone angle calculated in the CONTAM computer code<sup>19</sup>. The assumption was made that the plume interparticle collision frequency could be described by the classical statistical Boltzmann approach using densities, mean free paths, and collisional cross sections. Probably the least valid assumption was that the collisional processes were independent of the electrical forces or turbulent vortices. This is obviously not true, but as a first rough approximation, to be

---

21. Personal communication with Ron Kessler, NASA, MSFC, Oct. 1977

improved by later integration of the three models in a more rigorous model, it was judged expedient in order to permit solution of the independent models.

The approach was essentially statistical in nature. A Lambertian distribution of rebound directions was used to predict the impingement location. The location of the collision was given in cylindrical coordinates as  $(r_1, \theta_1, z_1)$  and the particle rebounded at the classical velocity given by a totally elastic collision to a position  $(r_2, \theta_2, z_2)$ . An integral was derived which gave the deposition expected at Point 2 resulting from collisions at all Points 1 incorporating all the assumptions of the model. This equation is:

$$\begin{aligned}
 M = & \int_0^t dt \int_{z_2'}^{z_2''} dz_2 \int_{M_{\text{MIN}}}^{1/10 M_{\text{MAX}}} dM_1 \int_{M_1}^{M_{\text{MAX}}} dM_2 \int_{v_{\text{MIN}}}^{1/2 v_{\text{MAX}}} dv_2 \int_{2v_2}^{v_{\text{MAX}}} dv_1 \int_0^{r_1'} dr_1 \int_{r_N}^{r_N + r_1 \tan \varphi} dz_1 \\
 & \times \left( \frac{8kT}{\pi \mu} \right)^{1/2} \left( \frac{\pi (d_1 + d_2)^2}{4} \right) \frac{N(M_1) N(M_2)}{\pi^2 (r_N + z_1 \tan \varphi)^4 v_1 v_2 t^2} \\
 & \times G(v_1, v_2) \quad V(r_1, \theta_1, z_1, r_2, \theta_2, z_2)
 \end{aligned} \tag{4}$$

where

$t$  = time  
 $(r_1, \theta_1, z_1)$  = collision location  
 $(r_2, \theta_2, z_2)$  = impingement location  
 $r_N$  = nozzle radius  
 $m_1$  = mass of smaller particle

$m_2$	= mass of larger particle
$m_{\min}$	= minimum mass of particles
$m_{\max}$	= maximum mass of particles
$v_1$	= velocity of smaller particle
$v_2$	= velocity of larger particle
$v_{\min}$	= minimum velocity of particles
$v_{\max}$	= maximum velocity of particles
$k$	= Boltzmann constant
$T$	= temperature
$d_1$	= diameter of smaller particle
$d_2$	= diameter of larger particle
$N(m)$	= number of particles of mass $m$
$\varphi$	= maximum angle of particle effluents
$\mu$	= reduced mass of two particles
$G(v_1, v_2)$	= bimodal Gaussian for particle velocities
$V(r_1, \theta_1, z_1, r_2, \theta_2, z_2)$	= Vector quantity dependent on Geometry

The computer analysis flow chart is indicated in Figure 8. This integration resulted in the total mass impingement on the spacecraft surfaces. The results as summarized in Figure 10 show no expected contamination from collisional processes.

This model is fundamentally limited by its assumption, but all attempts were made to keep it conservative. It is, however, a valid first approximation, being a conservative approach that was at the same time based upon realistic parameter values. Further refinements will include more exact modeling of the spacecraft and better data on adhesion. However, by far, the most important refinement of the model will be the integration of the three mechanisms; collisional, charge separation, and boundary flow effects to give a more realistic coupled mechanism which should predict the contamination more exactly.

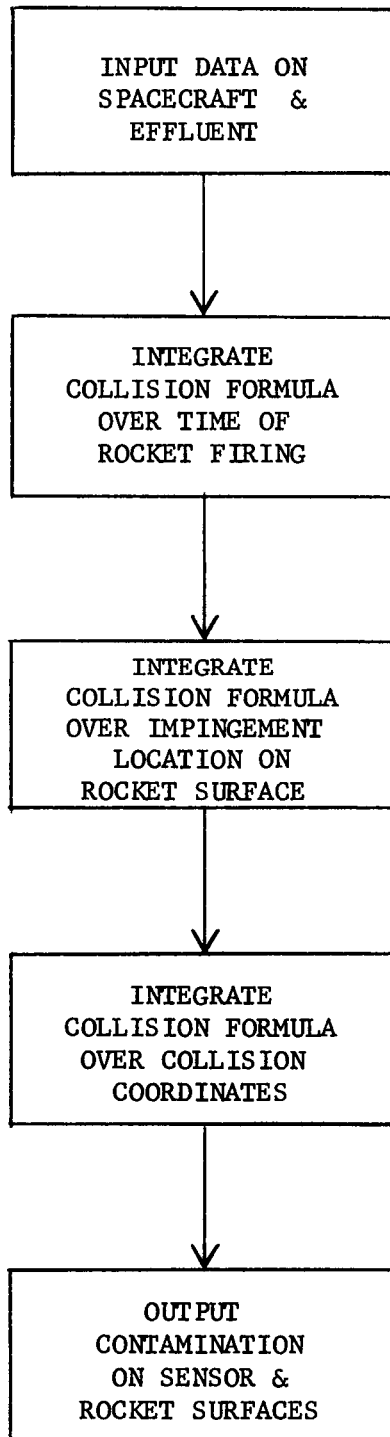


FIGURE 8 ANALYSIS FLOW CHART

### 3.3 Boundary Flow

The boundary-flow model consists of two parts. First a number of different mechanisms are invoked to explain migration of material to regions surrounding the upstream portion of a vehicle. The mechanisms are examined to determine how this material is directed towards the critical surfaces.

A number of assumptions and simplifying postulates were made to permit development of this model. They are summarized below:

A vacuum environment of  $10^{-8}$  Torr  $< P_{\text{ambient}} < 10^{-6}$  Torr was assumed and all possible influences from ultra-violet or other radiation were ignored. The surfaces were treated as if they were at uniform surface temperatures and all materials which collided with the critical surfaces were assumed to remain. For simplicity, the targets were treated in the same manner as the previous models; ideal cylindrical surfaces in accordance with the dimensions in Figures 5, 6 (cylinder No. 1 being closest to the SRM nozzle). Of the products of combustion, only  $\text{Al}_2\text{O}_3$ , considered as despositing. All other gaseous products are neglected. It was further assumed that the contaminant deposits are homogeneous and their distribution is uniform on any given idealized cylinder. The deposit density was taken as that of alumina and is in the range 3.5 to 3.9 gm/cm<sup>3</sup> <sup>22</sup>.

In addition, the following conditions were postulated: Flow is turbulent in the boundary layer and the fluid is compressible, viscous, and exhibits slightly non-Newtonian properties. Particles were assumed spherical of a maximum size of  $3\mu$  <sup>23</sup>. This general size

22. Goldsmith, A. and Waterman, T.E., Thermophysical Properties of Solid Materials, Armour Research Foundation WADC-TR-58-475 (1958).

23. Schorr, Morton, Solid Rocket Technology, Wiley (1972).

differs from that selected for the previously described mechanisms because of the manner in which they are generated by the exhaust<sup>\*</sup>. All collisions were treated as elastic. Only the steady-state condition was considered. The engine chamber pressure-time curve during firing was assumed constant over the steady state burn phase. The nozzle was assumed (for simplicity) to be conical instead of contoured and the nozzle half angle was taken as 15°. From the propellant weight and firing time it was estimated that the resulting average mass flow  $\bar{w} = 137.18$  lb/sec.

Starting with a clean nozzle, deposits are postulated to build up quickly on the nozzle walls up to a limiting thickness. This is supported both by experimental evidence and analysis as reported by Colucci<sup>24</sup>. It is believed that the phenomenon is the result of a steady-state condition established by virtue of the deposition of new materials and the simultaneous removal of already deposited material by the flow at the wall. This activity which takes place within the boundary layer where the velocities are relatively low, develops a mass fraction, constituted of relatively large particles, which is a combination of the masses normally present from the exhaust products plus the contributions being made by the material removed from the surface. The flow subsequently becomes fully turbulent<sup>25,26,27</sup> at the nozzle walls with a boundary layer thickness described by the following equation.

<sup>\*</sup>See discussion Pg. 25 on constitution of boundary layer.

24. Colucci, S.E., 5th Symposia on Ballistic Missile and Space Technology.

25. Skelland, A.H.P., Non Newtonian Flow and Heat Transfer, Wiley (1967).

26. Davies, J.T., Turbulence Phenomena, Academic Press (1972).

27. Marseille, Gordon, The Mechanics of Turbulence, International Symposium of The National Scientific Research Center, (1961).



$$\delta_T = \left\{ \frac{(\beta n + 1)\Omega}{\psi} \left[ 8^{n-1} \left( \frac{3n+1}{4n} \right)^n \right]^\beta (N_{Re,x}^o)^{-\beta} \right\}^{\frac{1}{\beta n + 1}} \quad (5)$$

The terms of this equation are defined by the following

$$\Omega = \frac{\alpha(0.817)}{z^{\beta n + 1}} 2^{-\beta(2-n)}$$

$$\psi = \frac{2-\beta(2-n)}{2(1-\beta+\beta n)} - \frac{2-\beta(2-n)}{2-2\beta+3\beta n}$$

$$N_{Re,x}^o = \frac{x^n u_o^{2-n} \rho}{K} \quad (\text{a form of Reynolds number for Non-Newtonian fluids})$$

for a Newtonian fluid  $n=1$  and  $K=y$

$$\text{and } N_{Re,x} = \frac{\rho u x}{y}$$

where  $u$  = velocity

$n$  is a "flow behavior index" for a non-Newtonian fluid where  $0 \leq n < 1$

$K$  is a "consistency" index analogous to viscosity

$x$  - distance along the surface

$f$  (friction factor in turbulent flow thru smooth tubes)

$$f = \frac{\alpha \gamma_1^\beta}{D^{\beta n} v^{\beta(2-n)} \rho^\beta}$$

$$\gamma_1 = 8^{n-1} K \left( \frac{3n+1}{4} \right)^n$$

$\alpha$  &  $\beta$  are defined as functions of  $n$

$D$  = tube diameter

$V$  = mean linear velocity

If the nozzle is considered as a very thin plate, the subsonic flow in the boundary layer (with a low  $\gamma$  of 1.13-1.3)<sup>27</sup> exhausts into a very high vacuum, under which conditions, compressible flow theory allows a turning angle for the flow of up to 180°. Associated with the back flowing material is a distribution of various combustion products with a total mass, mole fraction and consequent number of particles exhausting at a given instant. If the instantaneous mass flowing through the boundary layer thickness at the nozzle exit plane is summed over the total firing time, the total recirculated mass due to this mechanism results.

In addition, since the fluid is in reality not inviscid<sup>9</sup>, there will exist a transition fluid layer between the turbulent flow boundary layer and the free stream. In this transition region, particles will be experiencing high rotation,<sup>12,29,30</sup> resulting in the creation of a

<sup>28</sup>(1974): Thompson, Philip A., Compressible Fluid Dynamics, McGraw Hill

29. Hoglund, Richard F., Recent Advances in Gas Particle Nozzle Flows, ARS Journal, 32:662-671 (1962).

30. Tchernov, Alexander, Izvestiyn Akademii Nauk Kazakhskoi (SSR), Scriga Energetich, #8 (1955).

torus or vortex ring at the nozzle exit plane<sup>31,32</sup>. This grows to a certain size and provides a contamination source via one of two possible mechanisms: (1) the toroid separates from the main stream and migrates upstream, where it dissipates and forms a contaminant cloud,--these toroids are periodically formed during the entire firing time; (2) the toroid spalls off materials tangentially as it is being continuously fed by the exhaust products--some of the material having the appropriate vector velocity constitute the back flow contamination potential. For purposes of this study the former (migrating toroid) mechanism runs was invoked in evaluating the model. If the instantaneous masses in the toroids are summed over the firing time, total mass attributable to this mechanism results. Subsequent studies will deal with a steady -state torus expelling material into the backflow region.

Several additional phenomena may come into play to augment the back flow of the potential contaminants. For example, the effects of the high velocities, the step geometries at the nozzle edge, and the density distributions can generate severe curving shock waves in this regime.<sup>13</sup> These shock waves may act to direct the effluents in the reverse flow direction. Also, recent experimental and analytical evidence indicates that significantly greater mass fluxes than heretofore suspected exist at the Prandtl-Meyer limiting stream line of the plume<sup>8,9</sup>.

For the model under investigation, here, the mass contributed by this mechanism is derived as follows: a gas density distribution function is given by

$$f(\theta) = f(\theta_o) e^{-\beta(\theta-\theta_o)} \quad (6)$$

31. Prandtl, Ludwig and Tietjens, O.G., Fundamentals of Hydro and Aerodynamics, Dover (1957).

32. McCormack, Percival D., Vortex Ring and the Plate Jet, AIAA Journal, (April 1969).

where it is assumed that the streamline at the edge of the boundary layer turns through some angle  $\theta_0$ . The equation is valid for  $\theta > \theta_0$ . For  $0 < \theta < \theta_0$  a cosine law was proposed and is given by

$$f(\theta) = \cos^{\left(\frac{2}{\gamma-1}\right)} \left[ (\pi/2)(\theta/\theta_\infty) \right] \quad (7)$$

where

$\theta_\infty$  is the value of the limiting angle,  $\theta_\ell$ ,  
for inviscid supersonic flow

$\beta$  and  $\theta_0$  are functions of the nozzle exit condition and are given by

$$\beta = A[\gamma+1]/(\gamma-1)^{\frac{1}{2}} (2 \bar{U}_\ell/U_\ell) (R_e/2\delta)^{\frac{\gamma-1}{\gamma+1}} \quad (8)$$

where A is a constant and corresponds to a normalization factor for plume density given by:

$$A = \frac{U^*/2U_\ell}{\int_0^{\theta_\ell} f(\theta) \sin \theta \, d\theta}$$

in which  $U^*$  is the sonic velocity,  $U_\ell$  is the limiting velocity of the gas defined by

$$U_\ell = [(\gamma+1)/(\gamma-1)]^{\frac{1}{2}} U^*$$

and  $\theta_\ell$  is the limiting turning angle of gas at the nozzle exit.

$\theta_0$  is approximated by

$$\theta_\infty \left[ 1 - (2/\pi(2\delta/R_e))^{\frac{\gamma-1}{\gamma+1}} \right]$$

The mass flow in the portion of the plume defined by the above is given by

$$dm = -2\pi R_e (\rho U / \rho_e U_e)_{B.L.} \rho_e U_e dy \quad (9)$$

where  $y$  is location of the streamline from the nozzle wall

$\rho$  = gas density

whereas mass flow in the plume is expressed by

$$dm = \rho (\bar{U}/U_{\ell}) U_{\ell} 2\pi r^2 \sin \theta d\theta \quad (10)$$

$r$  = spherical radius from a point source  
with the nozzle

The mass backflow from this mechanism is evaluated by summing Equation (9) over the  $y$  and the firing time.

Since fluxes described by the exponential density distribution occur in the plume far-field at stream angles greater than  $90^\circ$  from the flow axis, their presence yields a rearward flow of material which interacts with already rearward moving existing material (see above), thereby increasing the potential for recirculation contamination. It should be noted that the above postulated mechanisms hold only during vacuum operation of the engines.

The basic analytical procedure is to determine the number of particles resulting in the masses generated by the various mechanisms identified above. Portions of the particles in each mechanism will fly off into space and not affect vehicle surfaces. Other particles will deposit according to mechanisms described below.

One of the driving mechanisms is the influence of existing electric fields. Soo<sup>33</sup> derives equations for a large number of uniformly charged solid particles. For a particle initially at radius R

$$v \frac{dv}{dr} = \frac{1}{\epsilon_o} \frac{q}{m}^2 \frac{M_R}{4\pi r^2} - \frac{12}{\rho_p \epsilon_o} \frac{\epsilon_r^{-1}}{\epsilon_r + 2} \frac{q}{m}^2 \frac{M_R^2}{(4\pi)^2 r^5} \quad (11)$$

Another of the driving mechanisms is collisions with existing products built up by toroidal migrations for which a mean free path is calculated:

$$\lambda_B = \frac{1}{\pi \sum_C n_C d_{BC} \sqrt{1 + \frac{m_B}{m_C}}} \quad (12)$$

33. Soo, S.L., Fluid Dynamics of Multiphase Systems, Blaisdell Publishing Co. (1967).

where

- n - number density of appropriate exhaust product  
i.e., specie C
- d<sub>BC</sub> - avge. molecular diameter of combined product
- m - molecular weight of each specie
- λ<sub>B</sub> - mean free path for specie B

From the point of impact, a particle/molecule is assumed to be reflected in a Lambertian distribution. The return flux through a 2 steradian solid angle is determined by calculating molecular column densities in a series of annular volumes at various radii from the spacecraft. The boundary flow Analysis Flow Chart is shown in Figure 9.

From the results of the boundary flow model, summarized in Figure 10, it can be seen that a significant amount of contaminant impingement can occur on the various surfaces. These calculations represent a severe understatement of the contamination potential in view of the very conservative assumptions made in the model. As in the case of the charge separation model, the true contamination picture requires integration of all the models and would probably yield higher deposits.

#### 4.0 RESULTS AND DISCUSSION

The summary of the results of the analytical model is presented in Figure 10. If simple additivity of the contributions from the mechanisms is assumed, the total contribution deposited on cylinder 6 (which can represent a critical payload area)  $16 \times 10^{-7} \text{ gm/cm}^2$ , would be unacceptable for systems as described in the introduction. It is, of course, recognized that the assumption of homogeneous deposition is questionable. However, there are both space and laboratory experimental indications that condensable products as well as superfine particulates may constitute a fair fraction of the recirculated product and thereby both behave as condensables to provide a relatively homogeneous deposit.

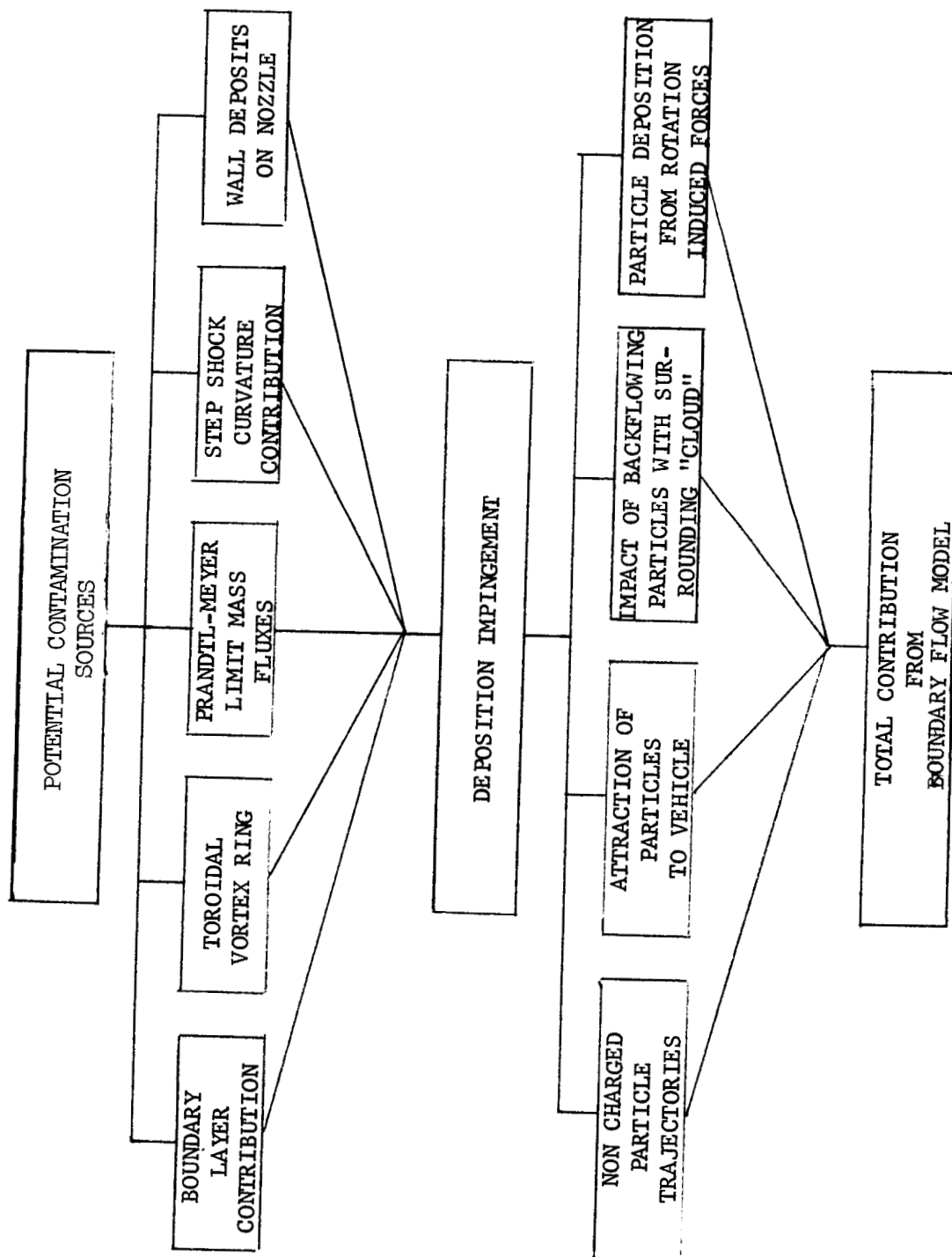


FIGURE 9 BOUNDARY FLOW ANALYSIS FLOW CHART



MODEL	IMPINGEMENT ( $\text{gm/cm}^2 \cdot 10^{-7}$ )					
	<u>CYL. 1</u>	<u>CYL. 2</u>	<u>CYL. 3</u>	<u>CYL. 4</u>	<u>CYL. 5</u>	<u>CYL. 6</u>
<b>Charge</b> Separation	62	45	28	17	9	5
Collisional	negl.	negl.	negl.	negl.	negl.	negl.
Boundary Flow	150	150	140	107	71	11
TOTAL	212	195	168	124	80	16

FIGURE 10 ACCUMULATIVE IMPINGEMENT

The conservative nature of the approach becomes evident when it is realized that none of the individual mechanisms account for the possibility of recirculated condensables. Furthermore, integration of the mechanisms into a consolidated model (rather than an additive model) would introduce cross coupled terms in the equation which would increase the calculated contamination. In addition, the contribution from the start-up and shut-down phases of the SRM burn would further increase the actual recirculation contamination potential over that estimated for the steady-state phase.

Questions have been raised regarding the rate of charge dissipation on a particle in a rocket plume plasma and it has been mentioned that particles would indeed have to recirculate on the order of a millisecond in order to impinge on sensitive surfaces before losing their charge. In fact, times of recirculation have generally been calculated to be less than a millisecond. The question has subsequently been postulated that prohibitively high velocities would have to be attained in order for particles to recirculate in such a short period of time. Velocities of that magnitude and much greater were calculated in the computer program and it is felt that these high velocities are in fact physically attainable by the particles. A plasma sheath due to atmospheric ionizing collisions with the surface of the spacecraft was not taken into account in this model. At the altitudes of interest this phenomenon may not be a substantial effect. Further investigation is warranted to see if in fact it will be present and, if so, to determine whether its effect is substantial or minimal.

However, the first SRM is fired in the ionosphere in a region where the ambient ion density is quite high. It is therefore likely that if a charge were to develop on the rocket surface that the field lines would be terminated on the ions present and that the particles emitted from the exhaust of the SRM would not even be influenced by these field lines. However, the effectiveness of the ambient ions in shielding the plume from the surface charge is related to the total voltage on the surface. From literature research it is estimated that the voltage on the spacecraft could be as much as a half million volts.<sup>10,11</sup> With voltages of this magnitude the Debye lengths are on the order of several meters and could indeed affect recirculation. Further models will take the effect of the ionosphere more rigorously into account but in this preliminary study it was felt that it would not substantially alter results. It is also true that the second rocket is fired at sufficiently high altitude to be out of the ionosphere and thus greater recirculation from electrical forces is anticipated. Its closer proximity to sensitive surfaces will also be a factor.

The question regarding the likelihood of the adherence of the aluminum oxide particles impacting the critical surfaces should be considered. First, it is obvious that the particles, if they do recirculate, will be hot from the combustion in the rocket and may have sufficient thermally-derived kinetic energy so that collisions would not be "sticky." Whether or not the particles can radiate sufficient energy in transport from plume to satellite so that sticking would occur is not evident without refinement of the analytical models. Alternately, the assumption of charge effects and van der Waals forces could account for the adherence of the particulates. Also a "fly-paper" effect from contaminants initially present on the critical surfaces might augment the adhesion. It might be expected that cold target surfaces could retain the contaminants more

effectively than warm surfaces so that the accumulative recirculation contamination effects might only be observed on the former. In the last analysis, since space flight evidence strongly indicates that recirculation contamination does occur, some effect or combination of the described effects must account for the observed contamination phenomena.

Preliminary joint efforts by the Aerospace Corporation and Aerojet were carried out to experimentally verify recirculation with both small SRMs and the full scale IUS motor in vacuum chambers at Arnold Engineering Development Center. The results,<sup>34</sup> while inconclusive, did demonstrate the presence of aluminum oxide, carbon and other, as yet, unidentified apparently condensable products forward of the nozzle end. However, questions concerning the validity of the results in the test chamber led to the conclusions that the question of recirculation contamination potential of SRMs will have to be resolved either with further refined laboratory testing or in an actual instrumented space flight. These possibilities are being actively pursued and further preliminary laboratory testing will be considered for the development of appropriate instrumentation.

The authors wish to graciously acknowledge the support of the Air Force program F04701-77-C-0010, under which portions of this information were developed. In addition, special thanks are given to E. Borson of the Aerospace Corporation for his contributions and participation in the program described.

34. Maag, Carl R., and Scott, R.R., Ground Contamination Monitoring Methods, presented at the USAF/NASA International Spacecraft Contamination Conference, Colorado Springs, Colorado (1978).

## 5.0 REFERENCES

1. Maag, Carl R., Backflow Contamination For Solid Rocket Motors, presented at the USAF/NASA International Spacecraft Contamination Conference, Colorado Springs, Colorado (1978).
2. Boynton, F.P., Exhaust Plumes From Nozzles With Wall Boundary Layers, Journal of Spacecraft & Rockets, 5:1143-1147 (1968).
3. Simons, G.A., Effect of Nozzle Boundary Layers in Rocket Exhaust Plumes, AIAA Journal, 12:718-720 (1974).
4. Pearce, Blain E., An Approximate Distribution of Mass Flux in a High Altitude Solid Propellant Rocket Plume, AIAA Journal, 12:718-720 (1974).
5. Arnold, F., An Experimental Method For Locating Stream Tubes In A Free Jet Expansion to Near Vacuum, AEDC-TR-69.17.
6. Seubold, Jason G., Edwards, R.H., A Simple Method For Calculating Expansion Of A Rocket Engine Nozzle Boundary Layer Into A Vacuum, Hughes Co.
7. Martinkovic, P.J., Bipropellant Attitude Control Rocket (ACR) Plume Contamination Investigation AFRPL-TR-69-261.
8. Chirivella, Jose E., Molecular Flux Measurements In The Back-flow Regions Of A Nozzle Plume, Tech memo 33-620, 1973, JPL.
9. Calia, U.S. and Brook, J.W., Measurements Of A Simulated Rocket Exhaust Plume Near The Prandtl Meyer Limiting Angle, Journal Spacecraft and Rockets, 12(No. 4): 205-208 (1975).
10. Fristrom, R.M., Oyhus, F.A., and Albrecht, G.H., Charge Buildup on Solid Rockets As A Flame Burst Mechanism, ARS Journal, 32:1729-1730 (1962).
11. Nanevicz, J.E., and Hilbers, G.R., Titan Vehicle Electrostatic Environment, Technical Report AFAL-TR-73-170, July 1973.
12. Smith, Felix T., and Gatz, Carole R., Chemistry of Ionization In Rocket Exhausts, Paper presented at the ARS Ions In Flows And Rocket Exhausts Conference, Palm Springs, CA. (1962).
13. Weinbaum, Sheldon and Weiss, Robert F., Hypersonic Boundary Layer Separation and The Base Flow Problem, AIAA Journal, 4 (No. 8): 1321-1330 (1966).
14. Grimson, J., Advanced Fluid Dynamics and Heat Transfer, McGraw Hill, 1971.
15. Private communication with M. Fong et al, Lockheed Missiles and Space Division, Sunnyvale, CA.

16. Cole, B.N., Baum, M.R., Mobbs, F.R., An Investigation of Electrostatic Charging Effects In High-Speed Gas-Solids Pipe Flows, Proceedings of The Institute of Mechanical Engineers, 184 (pt. 3C): 77-83 (1969).
17. Maise, George, and Sabadell, Albert J., Electrostatic Probe Measurements In Solid Propellant Rocket Exhaust, AIAA Journal, 8 (No. 5): 895-901 (1970).
18. Personal communication with E. Borson, Aerospace Corp., Nov. 1977.
19. Kliegel, James R., Gas Particle Nozzle Flows, Chemical Reactions and Phase Changes in Supersonic Flow.
20. Hoffman, R.J. et al, Plume Contamination Effects Prediction: The CONTAM Computer Program Version II, AFRPL-TR-73-46 (1973) Final Report, Contracts F04611-70-C-0076 and F04611-72-C-0037, McDonald Douglas Astronautics Corp.
21. Personal communication with Ron Kessler, NASA/MSFC, October 77.
22. Goldsmith, A. and Waterman, T.E., Thermophysical Properties of Solid Materials, Armour Research Foundation, WADC-TR-58-475 (1958).
23. Schorr, Morton, Solid Rocket Technology, Wiley (1972).
24. Colucci, S.E., 5th Symposia and Ballistic Missiles and Space Technology.
25. Skelland, A.H.P., Non Newtonian Flow and Heat Transfer, Wiley (1967).
26. Davies, J.T., Turbulence Phenomena, Academic Press (1972).
27. Marseille, Gordon, The Mechanics of Turbulence, International Symposium of The National Scientific Research Center (1961).
28. Thompson, Philip A., Compressible Fluid Dynamics, McGraw Hill (1974).
29. Hoglund, Richard F., Recent Advances In Gas Particle Nozzle Flows, ARS Journal, 32:662-671 (1962).
30. Tchernov, Alexander, Izvestiyn Akademii Nauk Kazekhskoii (SSR), Scriga Energetich, #8 (1955).
31. Prandtl, Ludwig and Tietjens, O.G., Fundamentals of Hydro and Aerodynamics, Dover (1957).
32. McCormack, Percival D., Vortex Ring and the Plate Jet, AIAA Journal, (April 1969).
33. Soo, S.L., Fluid Dynamics of Multiphase Systems, Blaisdell Publishing Co. (1967).
34. Maag, Carl R. and Scott, R.R., Ground Contamination Monitoring Methods, presented at the USAF/NASA International Spacecraft Contamination Conference, Colorado Springs, Colorado (1978).